Les Cahiers du GERAD ISSN: 0711–2440

Stope optimization with convexity constraints

G. Nelis, M. Gamache,
D. Marcotte, X. Bai

G–2015–47

May 2015

GERAD HEC Montréal
3000, chemin de la Côte-Sainte-Catherine
Montréal (Québec) Canada H3T 2A7

Tél. : 514 340-6053
Téléc. : 514 340-5665
info@gerad.ca
www.gerad.ca

Stope optimization with convexity constraints

Gonzalo Nelis [a]
Michel Gamache [b]
Denis Marcotte [c]
Xiaoyu Bai [b]

[a] *Department of Mining Engineering, Delphos Mine Planning Laboratory and Advanced Mining Technology Center, University of Chile, Santiago, Chile*

[b] *GERAD & Department of Mathematics and Industrial Engineering, Polytechnique Montréal, Montréal (Québec) Canada, H3C 3A7*

[c] *Department of Civil, Geological and Mining Engineering, Polytechnique Montréal, Montréal (Québec) Canada, H3C 3A7*

[d] *GERAD & Department of Civil, Geological and Mining Engineering, Polytechnique Montréal, Montréal (Québec) Canada, H3C 3A7*

gnelis@ing.uchile.cl
michel.gamache@polymtl.ca
denis.marcotte@polymtl.ca

May 2015

Les Cahiers du GERAD

G–2015–47

Abstract: A new algorithm for the optimal stope design problem is proposed. It is based on a previous methodology developed by Bai et al. (2013a) where a cylindrical coordinate system is used to define geomechanical restrictions and to find the optimal stope around an initial raise. The new algorithm extends this work using an Integer Programming formulation and a new set of constraints, aimed to solve geomechanical issues present on the original methodology. The new formulation is tested on two synthetic and one real deposits. An economic, geomechanical and feasibility analysis is performed, comparing the new results with Bai's methodology. This methodology achieves better stope designs in terms of geomechanical stability and wall regularity, generating feasible stopes for real use. It also allows further extensions to incorporate other geometrical constraints in order to obtain more regular stope designs.

Key Words: OR in mining, stope optimization, underground mining, sublevel stoping.

Résumé : Dans cet article, on propose un nouvel algorithme pour trouver le contour optimal des chantiers dans les mines souterraines. Il est basé sur une méthodologie développée précédemment par Bai et al. (2013a) où un système de coordonnées cylindrique est utilisé pour tenir compte des restrictions géomécaniques et de trouver le contour optimal d'un chantier autour d'une monterie. Le nouvel algorithme propose une extension de ce travail en utilisant un modèle de programmation linéaire en nombres entiers et une nouvelle série de contraintes, visant à résoudre les problèmes géomécaniques observés avec le modèle précédant. La nouvelle formulation est testée sur deux instances artificielles et un cas réel. Une analyse économique et géomécanique ainsi que sur la faisabilité est effectuée afin de comparer les nouveaux résultats à ceux obtenus avec la méthodologie de Bai. La nouvelle méthode permet d'obtenir une meilleure conception des chantiers en termes de stabilité géomécanique et des épontes plus régulières, et de générer des chantiers admissibles en pratique. Il permet également de nouvelles extensions qui permettraient d'incorporer d'autres contraintes géométriques.

1 Introduction

The main objective of underground mining is to achieve the highest profit from the orebody while maintaining a safe operation. For this, both economical and geomechanical factors have to be considered for the selection of the mining method and the design of the associated stopes. One of the most widespread underground mining system is "Sublevel Stoping", in which an open stope is created with dimensions according to geomechanical conditions of the rock mass, the selectivity desired and profitability of the stope.

Several methods have been proposed to address the underground design problem and they can be classified in 1D, 2D and 3D methods. Among the 1D and 2D methods, the most relevant are the dynamic programming algorithm (Riddle, 1977) and the branch and bound technique (Ovanic and Young, 1995), which find the optimal design but they do not consider the three dimensional nature of the problem. On the other hand, the most relevant 3D methods are the floating stope algortihm (Alford, 1996), the octree division algorithm (Cheimanoff et al., 1989), the maximum value neighborhood method (Ataee-Pour, 2000), and simulated annealing techniques (Manchuk and Deutsch, 2008). All these methods address the three dimensions, but they cannot generate an optimal stope design incorporating real geomecanichal restrictions. A comprehensive review can be found in (Ataee-Pour, 2005).

However, recent progress have been made on this subject for the case of sublevel stoping. In Bai et al. (2013a), the authors find the stope design that maximizes the profit obtained. Their approach is based on a transformation from the Cartesian coordinate system to a cylindrical system centered around the initial raise. The authors could define the optimal stope incorporating some geomechanical constraints as the footwall and hangingwall angles, the minimum stope width that ensures the flow of the blasted ore towards the raise, and the maximum distance from the raise to control the size of the final stope. This approach was extended to include multiple raises (Bai et al., 2014) and to incorporate drift development in the optimization process (Bai et al., 2013b). This problem can be solved using a network structure and an efficient maximum flow algorithm (Picard, 1976).

In regular deposits, this methodology generates feasible stope designs. However, on irregular deposits, the stope designs may present stability problems with irregular contours, despite the imposed restrictions of footwall and hangingwall angles.

The stope stability is defined based on the rock mass properties such as uniaxial or triaxial compressive strength, rock mass condition, presence of faults or structures, etc. (Bieniawski, 1989; Laubscher, 1990). To ensure the stability of a given stope it is necessary to define its shape, maximum dimensions, footwall and hangingwall angles and the global stope inclination (Mathews, 1980). The methodology proposed by Bai successfully incorporates the footwall and hangingwall angles and the stope maximum dimensions, but in some cases the stopes present shapes that reduce their global stability. Fig. 1 illustrates such a stope obtained with Bai's approach where stability problems may occur, resulting in increased ore dilution.

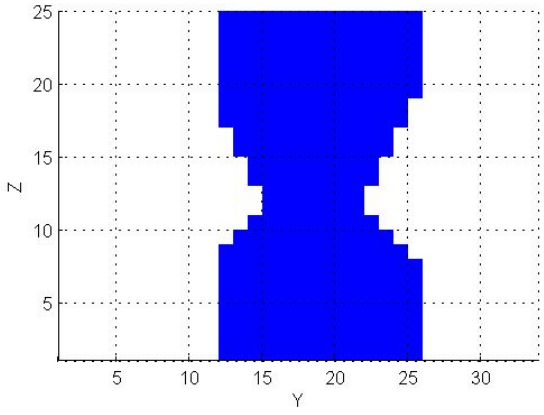

Figure 1: Stope generated by Bai's methodology, with stability issues. The stope is 12 meters width and 25 meters tall approximately. YZ vertical section at X=30.

In the next section, we briefly review the method used to measure stope stability. We show how the lack of convexity along the stope sides influence negatively the stability. We recall the main points of the approach used by Bai et al. (2013a). Then we describe the new linear program used to enforce convexity of the stopes. Finally, the results obtained with and without the convexity constraints are compared on a few simple synthetic deposits and a real deposit.

2 Methods

2.1 Stope stability determination

To study the stope stability, we use the strength factor defined as:

$$SF = \frac{RockMassStrength}{InducedStress} \tag{1}$$

Fig. 2 presents the strength factor obtained from a 2D stability analysis of the stope central cross-section.

The analysis is done using Examine2D (Roclab, 2014). The software implements 2D boundary elements analysis (Crouch and Starfield, 1983) to calculate the stress induced in the rock mass around the excavation. It assumes a linear elastic, continuous, isotropic and homogeneous rock mass and, of course, it neglects the 3rd dimension. Despite these strong assumptions and simplifications, the stability analysis remains useful to compare relative stability of different stope designs in a given rock mass.

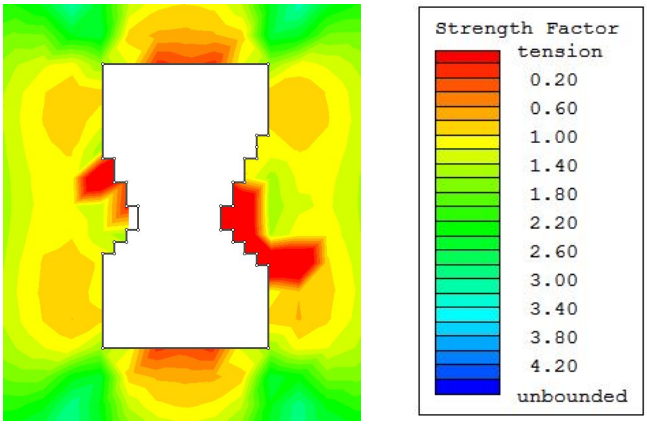

Figure 2: Stability analysis of stope generated by Bai's methodology, with stability issues. The midsection presents possible failure by tension

For simplicity, the failure criterion to calculate SF was Mohr-Coulomb (Coulomb, 1776), but any other failure criterion could be used. The midsection presents a possible failure by tension zone. This section will flow inside the stope, diluting the ore and reducing the stope profit. Hence, this design could be not optimal when considering the additional dilution. For comparison, a stope with the same dimensions is presented in Fig. 3 but with a straight midsection.

2.2 Model formulation

The proposed model is based on the Ultimate Pit Problem or Final Pit Problem in open pit mining (Lerchs and Grossmann, 1965). The objective is finding the part of the orebody which maximizes the profit obtained when it is extracted and processed. To achieve this objective, the original orebody is discretized in small blocks with different attributes such as metal content, extraction cost, processing cost, tonnage, coordinates, etc. From these attributes, an economic block model is defined using a profit function (Lane, 1988), where each block has a value representing the net profit of extracting that particular block. It is important to mention that the set of blocks extracted must ensure the pit wall stability, typically defined as a wall pit

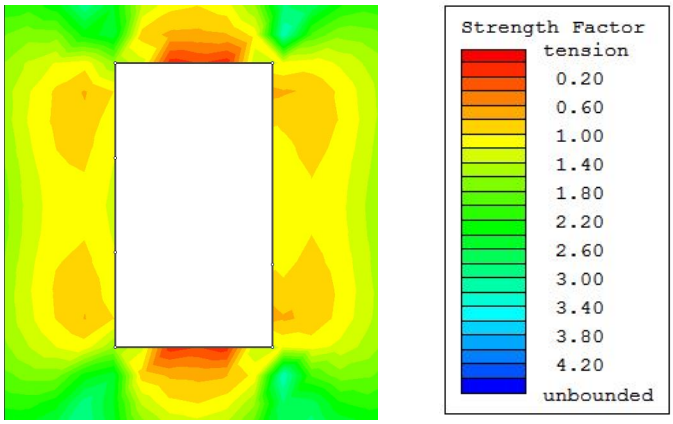

Figure 3: Stability analysis of a stope with the same dimensions as Fig. 2, but with a straight midsection. The previous tension zone presents a better stability.

angle. For this reason, geometrical precedence constraints are defined between blocks to maintain the required angle. Formally, this problem can be defined as a linear integer program:

$$\max \quad \sum_{i \in N} x_i p_i$$

$$\text{s.t.} \quad x_i \leq x_j \qquad \forall (i,j) \in \mathcal{P}_i \tag{2}$$

$$x_i \in \{0,1\} \qquad \forall i \in N \tag{3}$$

The variable x_i equals 1 if the block i in N is extracted and 0 otherwise. The parameter p_i is the extracting value of block i. The restriction set is derived from the precedence constraints between blocks to maintain the wall pit angle. The set $\mathcal{P}_i$ contains all ordered pairs (i,j) where block j must be extracted before block i. Finally, the objective is to find the set of blocks that maximizes the profit, subject to every block in this set must be extracted towards the surface fulfilling the precedences between blocks.

Similarly, in the sublevel stoping mining system, a vertical raise is drilled in order to create enough space to blast the ore inside the stope. The blasted material fills the raise and falls down by gravity towards the drawpoints located in the bottom of the stope. Sequential blasts are performed to extract all the material in the stope taking advantage of the new space created from former blasts. Therefore, the role played by this initial raise is analogous to the surface in open pit mining: All the blocks must move towards the raise/surface in order to be extracted. Hence, the precedences between blocks should link every block to the initial raise. This is the base for the cylindrical coordinate system transformation proposed by Bai et al. (2013a).

2.3 Cylindrical block model

In Bai et al. (2013a), an algorithm to transform a conventional block model (in the Cartesian coordinate system) into a cylindrical block model is proposed in order to emulate the role played by the ground surface in open pit mining with the initial raise in sublevel stoping. The raise is defined as the center of the cylindrical system, and a set of regular blocks are defined surrounding this raise from a discretization of Δr, $\Delta\theta$ and Δz defined by the user. This transformation presents a big advantage: to extract any block of the block model, diagonal links can be defined in the cylindrical system towards the raise, and this structure of links can be represented in the Cartesian coordinate system to generate the geometry shown in Fig. 4.

This figure shows that any block to be extracted forces all its predecessors towards the raise to be extracted too, emulating the desired behavior. Furthermore, using this transformation, the footwall and hangingwall angles can be defined directly with diagonal links as it is shown in Fig. 4c. Also, the discretization of Δr, $\Delta\theta$ and Δz can be chosen based on the footwall and hangingwall angles and the minimum stope width to allow a steady flow of material towards the raise. This problem can be solved using a network structure and efficient maximum flow or other algorithms.

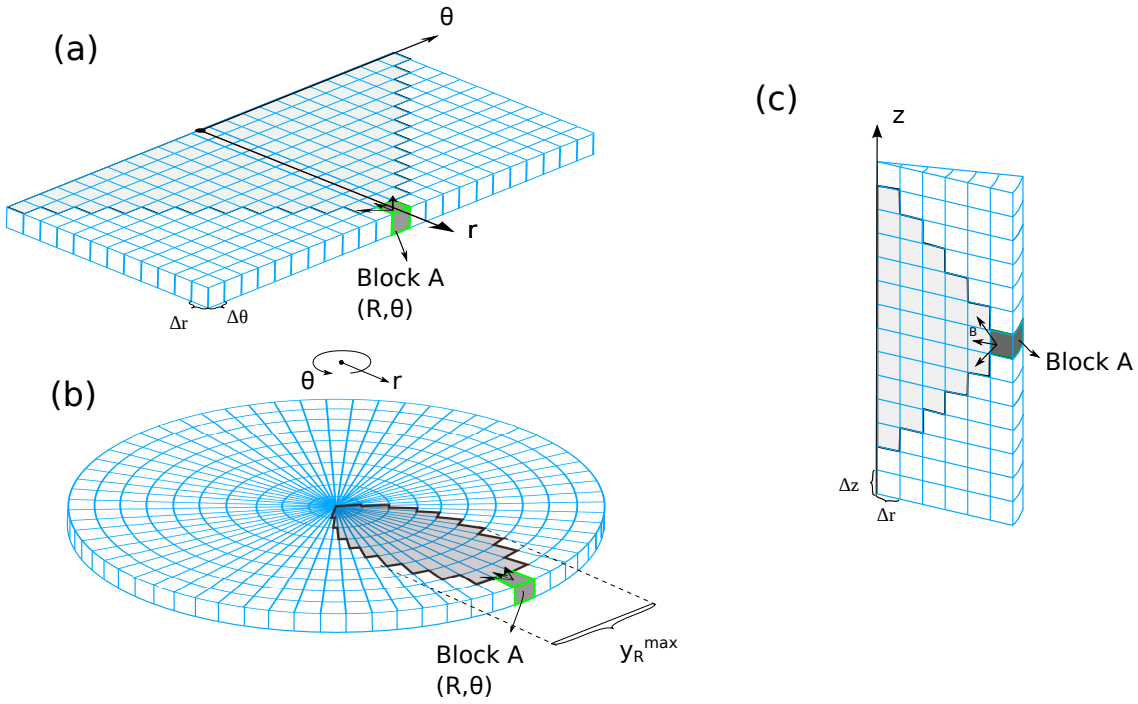

Figure 4: Horizontal precedences developed by Bai. Fig. (a) shows how this precedences are generated in the cylindrical system, and Fig. (b) shows this pattern in the Cartesian system. Shaded blocks are the blocks to be removed in order to extract the block A. Black point in the center represents the raise. Fig. (c) shows diagonal links in the cylindrical system to generate the footwall and hangingwall constraints

In this paper we will use the same transformation proposed by Bai et al. (2013a), with the same precedences of footwall and hangingwall angles and the minimum stope width. The raise location is considered known, but it can be optimized as in (Bai et al., 2014). This is the base used to improve the algorithm with the new constraints presented in the next section.

2.4 Stope convexity constraints

In order to avoid the irregular shapes in the stope outer section a possible solution is the creation of vertical precedences between the blocks of the block model in the cylindrical coordinate system. However, these precedences interfere with the footwall and hangingwall angle restrictions, generating a 90 degree angle despite the minimum angle imposed before.

For this reason, the restriction must be imposed in a different way. In Fig. 5, a single column from a block model is presented. To avoid non-convex geometries, we must consider that if a block from this column is extracted, and the block below is not, then all the blocks below must not be extracted. For instance, if block A is extracted and block B is not, all the blocks below B must not be extracted in order to avoid the generation of non-convex geometries. The advantage of putting the restrictions in this way is that it does not interfere with neither the footwall or hangingwall constraints because it does not force the vertical extraction in all situations.

For the implementation of this restriction, let define $C_{i,c}$ the set of all blocks in the block model inside the column c, and with a z coordinate lower than the z coordinate of block i. In other words, $C_{i,c}$ is the set of all blocks below the block i in a single column. A column is defined as the set of all blocks with the same r and θ coordinates, or the same x and y coordinates in the Cartesian system. The set of all columns in the block model is called C. With these definitions, the integer program to force convexity is shown:

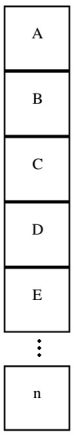

Figure 5: A single column of a block model

$$
\begin{aligned}
\max \quad & \sum_{i \in N} x_i p_i & & \\
\text{s.t.} \quad & x_i \leq x_j & \forall (i,j) \in \mathcal{P}_i & (4)\\
& x_j + \alpha_{j,c} \geq x_i & \forall\ \{(i,j) \mid j\ \textit{immediately below}\ i\} & (5)\\
& x_i \leq 1 - \alpha_{j,c} & \forall i \in C_{j,c} & (6)\\
& x_i, \alpha_{i,c} \in \{0,1\} & \forall i \in N, c \in C & (7)
\end{aligned}
$$

The decision variable x_i and the coefficient p_i have the same meaning as the final pit problem. The new binary variable, $\alpha_{i,c}$ is defined as 1 if all the blocks in column c and below the block i **must not** be extracted. To clarify this concept, an example using Fig. 5 is shown. Applying this restrictions to the first block in this column:

$$
\begin{aligned}
& x_B + \alpha_B \geq x_A & & (8)\\
& x_i \leq 1 - \alpha_B \qquad \forall i \in C_B = \{C, D, E, \ldots, n\} & & (9)
\end{aligned}
$$

In this case, if the block A is extracted, and at the same time, B is not extracted, restriction 8 forces the variable α_B to be 1. If this variable is 1, the right side in restriction 9 is 0, forcing all the blocks $i \in C_B$ to be 0, or, in other words, all the blocks below i must not be extracted. Both restrictions combined avoid the non-convexity issues presented before, ensuring a better stope shape. However, the addition of this new constraints with the new variable to the original problem generates the loss of the network structure. Therefore, this problem can not be solved using max flow algorithms. Branch and bound algorithms will be used instead, in order to find the optimum stope design. This algorithms are slower than max flow algorithms, hence the runtimes of this new problem will be studied as well.

3 Results

3.1 No convexity constraints

First of all we present the results obtained from the integer program implementation (IP formulation) without convexity constraints solved with simplex and branch and bound algorithm implemented in Gurobi 5.6.3. This problem is equivalent to the network problem solved by Bai with maximum flow algorithm, therefore, in order to validate the new implementation, we will compare the performance of both algorithms solving the same instance. A real orebody, presented in Fig. 6, will be used with the economical and geomechanical parameters shown in Table 1.

Table 1: Geomechanical, design and economic parameters for stope optimization algorithm

Parameter	value
Design and geomechanical parameters	
Stope width (m)	6
Footwall angle (deg)	60
Hangingwall angle (deg)	45
Economic parameters	
Unitary cost ($/unit)	50
Cut-off grade	0.005
Selling price ($/unit)	10
Recovery rate (%)	90
Density (unit/m^3)	2.3

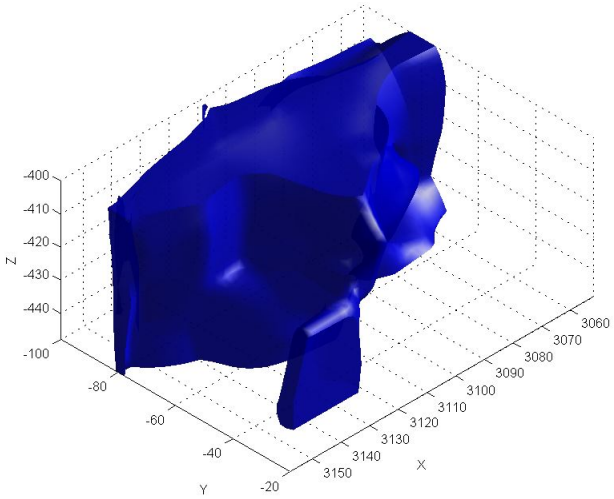

Figure 6: Real deposit used in this analysis

Also, with the aim to test the performance in bigger instances, the cylindrical block model discretization was changed, generating bigger block models which are more difficult to solve. The performance of both algorithms is presented in Table 2.

As it is shown in Table 2, both methods achieve practically the same results in terms of optimum stope design, with differences lower than 1% in every field. Particularly, in the profit field, the difference is less than 0.01%. This plays the role of objective function of both algorithms, therefore, both algorithms can be taken as equivalents. Fig. 7 presents a cross section of the stope obtained by both methods, and it can be shown

Table 2: Comparison between network structure - Flow algorithm and IP formulation - Gurobi simplex algorithm

$\Delta r/\Delta x$	Algorithm	Stope profit ($)	Missed ore($)	Waste cost($)	Dilution (%)	Runtime (s)
1	Flow	1,196,167	188,471	7,409	3.49	1.1
	Gurobi	1,196,230	188,374	7,433	3.52	3.5
0.5	Flow	1,194,611	190,574	6,862	3.21	7.7
	Gurobi	1,194,665	190,517	6,865	3.22	39.2
0.4	Flow	1,195,716	188,357	7,975	3.6	15.7
	Gurobi	1,195,738	188,310	7,999	3.6	68.3
0.3	Flow	1,198,698	185,316	8,034	3.59	39.9
	Gurobi	Out of memory error				

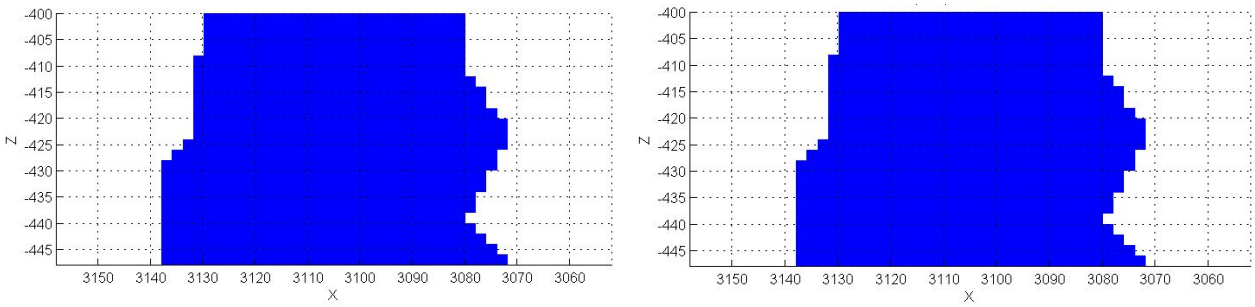

(a) Maximum flow (b) Gurobi

Figure 7: Vertical sections (Y=-68) of optimal stopes generated by maximum flow algorithm and Gurobi simplex algorithm

that the results are exactly the same. With this result, we validate the integer program implementation of Bai's methodology.

On the other hand, if we compare the runtime of both algorithms, the maximum flow implementation solves the same instances up to 5 times faster than Gurobi. However, for the integer nature of this formulation, the results obtained by Gurobi are notably fast. This is due the structure of these linear integer programs: the restriction matrix generated by all the precedence constraints is totally unimodular. Therefore, the linear relaxation of these instances, solved by simplex, generate an integer solution without using the branch and bound techniques. This property cause a runtime remarkably low compared to another instances with comparable size. Thereby, the IP-program implementation is still useful for solving these instances.

3.2 Convexity constraints

To study the effect of the convexity constraints proposed before, three different orebodies were used. The first one corresponds to the real deposit used in the previous section, presented in Fig. 6, and its results with the convexity constraints are presented in Table 3 along with the results obtained using Gurobi on the same instance without the new constraints, to compare both results graphically and quantitatively. In terms of value, for this orebody, the difference between both cases is less than 1%, with a small raise in the dilution inside the stope, and less ore recovery. This behavior is expected due the fact that the new constraints reduce the feasible region of the initial problem.

Table 3: Stope design results of IP-formulation for real deposit

$\Delta r/\Delta x$	Case	Stope profit (k$)	Missed ore (k$)	Dilution (%)
1	No convexity[a]	1,196	188	3.52
	Convexity (gap 0.1%)[b]	1,196	189	3.83
	Convexity (gap 0.01%)[c]	1,195	190	3.54
0.9	No convexity	1,195	189	3.60
	Convexity (gap 0.1%)	1,194	190	3.97
	Convexity (gap 0.01%)	1,193	191	3.70
0.8	No convexity	1,191	194	3.49
	Convexity (gap 0.1%)	1,191	194	3.78
	Convexity (gap 0.01%)	1,190	195	3.51

[a] No convexity: IP-formulation without convexity constraints
[b] Convexity (gap 0.1%): IP-formulation with convexity constraints. Minimum optimality gap: 0.1%
[c] Convexity (gap 0.01%): IP-formulation with convexity constraints. Minimum optimality gap: 0.01%

In relation to runtimes of both algorithms, the addition of the new constraints generates a significant increase of the solving time for the same deposit. This is due the fact that the restriction matrix is not totally unimodular under the new constraints, therefore the simplex solution is not integer and branch and bound techniques must be applied, with the notable increase in the time to deliver the optimum stope, being up to 34 times slower than the original formulation. In this regard, it is pertinent to emphasize the magnitude of this instance in terms of variables and constraints (see Table 4). Compared to the original formulation, the number of variables is doubled as it is expected, due to the new α variable. Also, the number of constraints increases up to 3.2 times, generating an instance of nearly 3 millions of constraints in the instance with the smallest discretization presented here.

Table 4: Optimization results of IP-formulation for real deposit

$\Delta r/\Delta x$	Case	Objective function (k$)	Optimality gap (%)	Constraints	Variables	Runtime (s)
1	No conv.[a]	104,160	-	484,390	73,944	3.7
	Conv.0.1[b]	104,034	0.0763	1,337,590	147,888	45.4
	Conv.0.01[c]	104,096	0.0088	1,337,590	147,888	47.7
0.9	No conv.	107,014	-	669,578	98,000	5.5
	Conv.0.1	106,913	0.0478	1,992,578	196,000	128.6
	Conv.0.01	106,946	0.0099	1,992,578	196,000	154.0
0.8	No conv.	105,675	0	920,033	138,688	8.1
	Conv.0.1	105,572	0.0563	2,935,343	277,376	229.4
	Conv.0.01	105,616	0.0092	2,935,343	277,376	280.4

[a] No conv.: IP-formulation without convexity constraints
[b] Conv.0.1: IP-formulation with convexity constraints. Minimum optimality gap: 0.1%
[c] Conv.0.01: IP-formulation with convexity constraints. Minimum optimality gap: 0.01%

For the synthetic deposits, two different cases are shown. The first deposit represents an adverse case for the original algorithm since it contains high value on top and bottom zones, and a narrow band in its center (Fig. 8a). This geometry generates a non-convex zone in its midsection. The second case, shown in Fig. 8b, represents a deposit with scattered high grade blocks through all the orebody, producing irregular contours. The results for both orebodies are presented in Table 5.

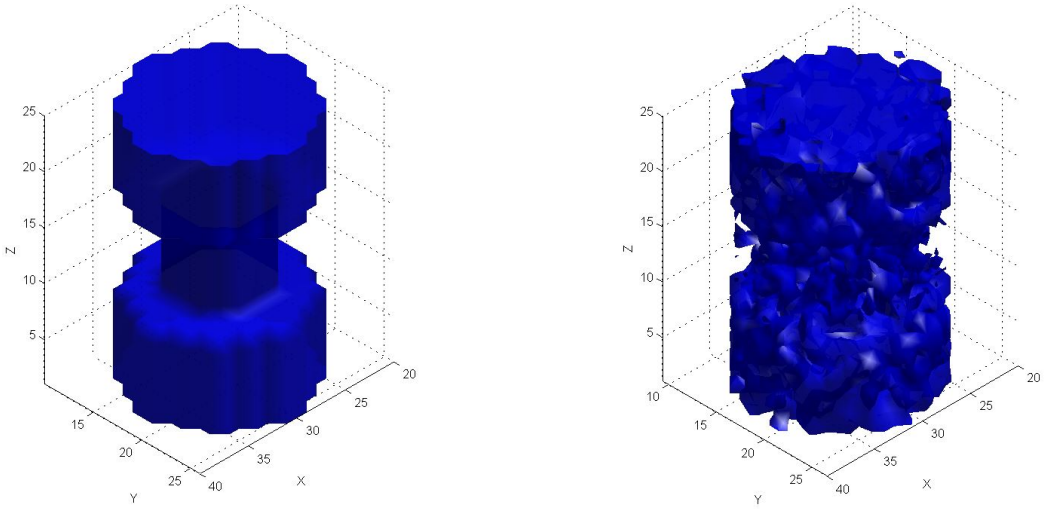

(a) Deposit 1 (b) Deposit 2

Figure 8: Isometric views of both synthetic deposits used in this analysis. Only blocks with positive profit value are shown

Table 5: Stope design results of IP-formulation for synthetic deposits

$\Delta r/\Delta x$	Case	Stope profit (M$/k$)	Missed ore (M$/k$)	Dilution (%)
		Deposit 1		
1	No convexity const.	402.5	87.8	22.5
	Convexity (gap 0.1%)	404.9	85.1	26.7
	Convexity (gap 0.01%)	403.8	86.3	26.2
0.5	No convexity const.	475.3	15.2	14.6
	Convexity (gap 0.1%)	472.7	17.1	27.6
		Deposit 2		
1	No convexity const.	7.24	0.86	28.2
	Convexity (gap 0.1%)	7.16	0.95	28.2
	Convexity (gap 0.01%)	7.16	0.95	28.2
0.8	No convexity const.	7.41	0.74	25.4
	Convexity (gap 0.1%)	7.27	0.78	29.4
	Convexity (gap 0.01%)	7.27	0.78	29.3

For both cases, the designs with and without convexity constraints present similar objective functions, with differences lower than 2%. However, dilution inside the stopes increases significantly, since the solution must add new waste blocks to meet the convexity constraints. In this regard the most critical case is deposit 1 with discretization $\Delta r/\Delta x = 0.5$, with an increase in dilution from 14% to 27%. This is because the smaller discretization allows a greater degree of selectivity in the original problem which is lost by using the new convexity constraints.

Moreover, it is relevant to mention that, in most cases, the addition of convexity constraints produces a greater amount of ore missed compared to the original solution. This can be interpreted as a trade-off between ore and value: in some zones of the deposit it is better to leave certain ore blocks out of the solution in order to meet the convexity constraints. Adding these extra ore blocks would add too much dilution to the solution.

The differences between the resolution time with and without convexity constraints vary greatly depending on the size of the problem (see Table 6). For the first deposit, for instance, with a discretization of $\Delta r/\Delta x = 1$, the runtime is doubled when convexity constraints are used. On the other hand, with a discretization of $\Delta r/\Delta x = 0.8$, the solving time is up to 23 times greater for the same deposit. This indicates the great

Table 6: Optimization results of IP-formulation for synthetic deposits

$\Delta r/\Delta x$	Case	Objective function (M$/k$)	Optimality gap (%)	Constraints	Variables	Runtime (s)
			Deposit 1			
1	No conv.	4,136.3	-	18,016	2,940	0.35
	Conv.0.1	4,128.9	0.0101	34,396	5,880	0.82
	Conv.0.01	4,129.0	0.0095	34,396	5,880	0.86
0.5	No conv.	4,931.5	-	128,144	19,656	2.51
	Conv.0.1	4,924.5	0.0079	354,944	39,312	14.83
			Deposit 2			
1	No conv.	68.6	-	18,016	2,940	0.34
	Conv.0.1	56.4	0.08	34,396	5,880	2.24
	Conv.0.01	56.4	0.001	34,396	5,880	2.68
0.8	No Conv.	69.2	-	33,922	5,406	0.63
	Conv.0.1	66.8	0.097	72,082	10,812	7.52
	Conv.0.01	66.8	0	72,082	10,812	14.88

impact of the instance size on the solving times. For example, despite being the same deposit, increasing the variables and constraints twice using a smaller discretization generates a solving time 8 times greater for the lowest gap shown in Table 6 for deposit 2: from 2.68[s] to 14.88[s].

3.3 Stope shape and stability

To study the stope stability on the new solutions, we compare different stope designs in Examine2D, showing the strength factor using Hoek and Brown (Hoek et al., 2002) and Mohr-Coulomb (Coulomb, 1776) failure criteria. The results for the real deposit (Fig. 9) are presented in Fig. 10. Those for the synthetic deposit (Fig. 11) are presented in Fig. 12 and Fig. 13. The parameters and geomechanical conditions used for these two analysis are presented in Table 7.

Table 7: Geomechanical and failure criterion parameters

Parameter	Value
Insitu stress parameters	
Depth (m)	450
Overburden unit weight (MN/m^3)	0.026
Horizontal stress ratio	1.5
Out of plane stress ratio	1.2
Rock mass strength parameters	
Tensile strength (Mpa)	0.3
Cohesion (Mpa)	2
Friction angle (deg)	50
High quality rock	
Intact compact strentgh (Mpa)	250
GSI	60
mi	25
Low quality rock	
Intact compact strentgh (Mpa)	100
GSI	20
mi	25

In Fig. 10, the original stope presented a non-convex zone in its corner, generating a failure by tension zone. The new stope, on the other hand, does not present that tension zone, achieving a greater stability in that corner. Furthermore, the stope stability in other zones also improves as we can see in the upper-left corner, where the original stope had an unstable zone that was improved significantly with the new constraints. The induced stress over this zone changes due to the regularization of the stope. Therefore, the convexity constraints can improve not only the local stability, but the global stability as well.

Similar observations can be made for the synthtic deposit (Fig. 12). The failure zone in the right middle part is substantially reduced with the new convexity constraints.

This behavior holds true for different rock mass qualities, as it can be seen in Fig. 13, where we evaluated the same stope geometry, under the same stress conditions, but with a low quality rock mass detailed in Table 7. Therefore, the new geometries generated by the convexity constraints are more stable than the stopes from the original methodology, independently of the rock mass quality.

4 Discussion

The new IP-formulation presented in this work improves the stope designs obtained by the network formulation by Bai et al. (2013a). The addition of the convexity constraints achieves more regular and geomechanically more stable shapes without using an additional step to manually regularize the stope borders with the risk of loosing the design optimality.

In the examples presented the stopes obtained under the new IP formulation are comparable with the stopes obtained by Bai's methodology, with very small differences between the stope profit function. However,

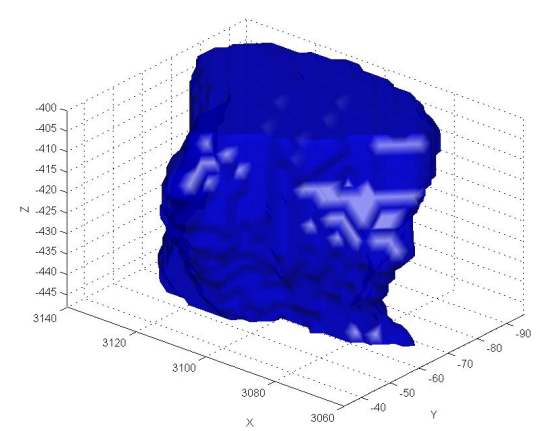

(a) Isometric without convexity constraints

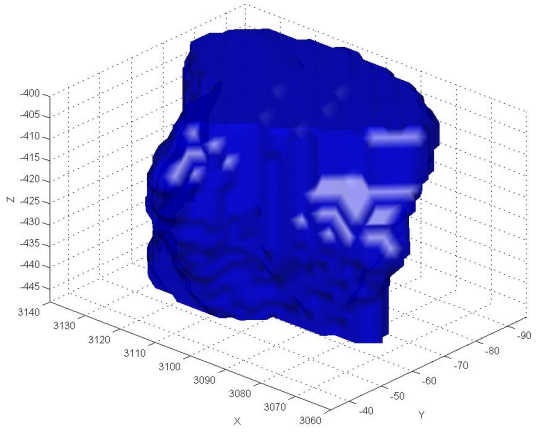

(b) Isometric with convexity constraints

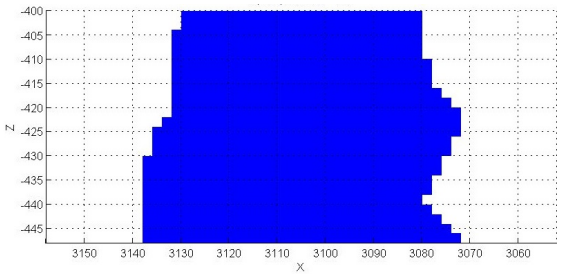

(c) Slice XZ (Y=-68) without convexity constraints

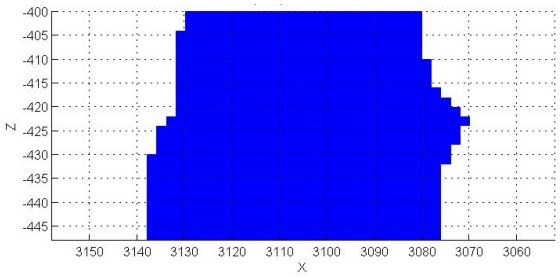

(d) Slice XZ (Y=-68) with convexity constraints

Figure 9: Stope shapes of both algorithms applied on real deposit

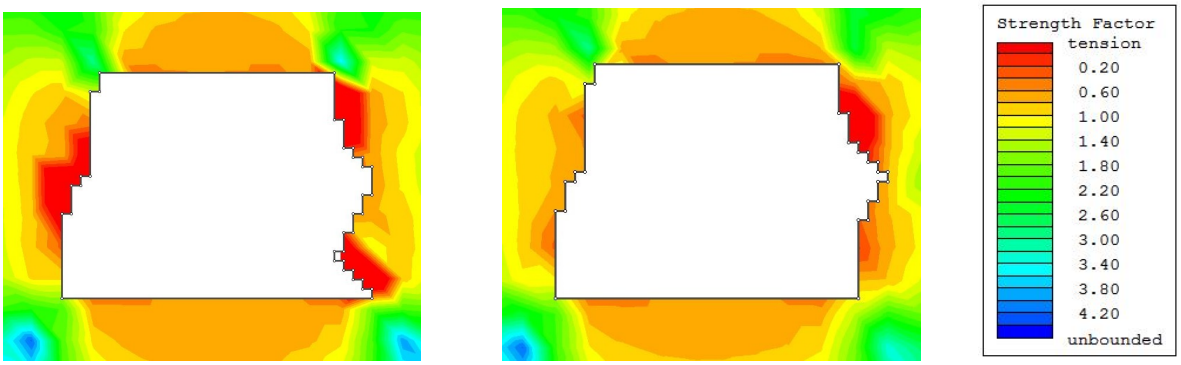

(a) Without convexity constraints (b) With convexity constraints

Figure 10: Stability analysis of a cross-section on real deposit stope

these results can not be extrapolated to other cases since they are problem dependent. Depending of the cost structure, the stope profit reduction could be greater with the IP formulation.

The block discretization and the back-transformation from cylindrical to Cartesian coordinates, necessary in Bai's approach, introduce some distortions in the final computed profits. Hence, in Table 3, the profit with a bigger optimality gap is larger, an unexpected result. Similarly in Table 5, the profit with the convexity constraints is slightly larger than without the constraints. These distorsions tend to diminish or disappear when the discretization in the cylindrical system is made finer. Their amplitude is small (less than 1% of the

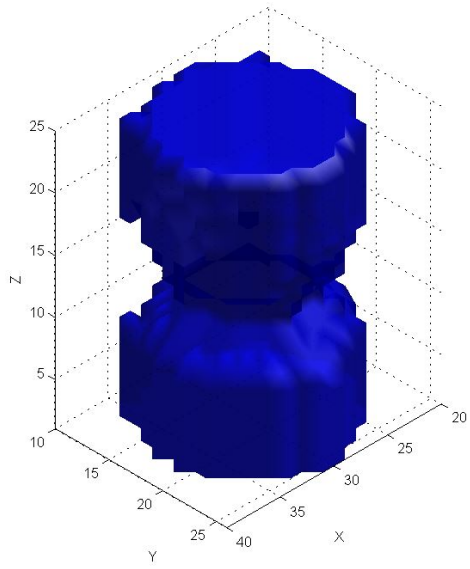

(a) Isometric without convexity constraints

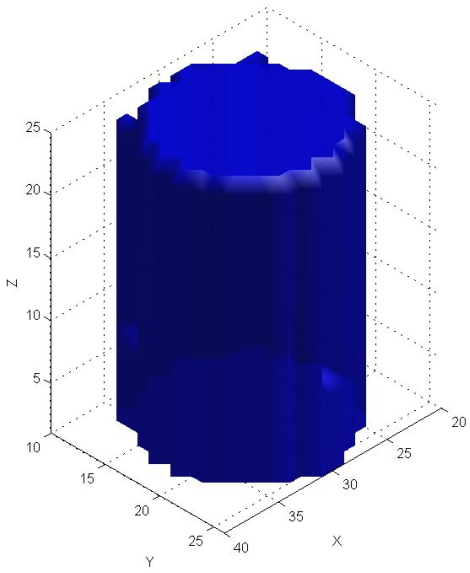

(b) Isometric with convexity constraints

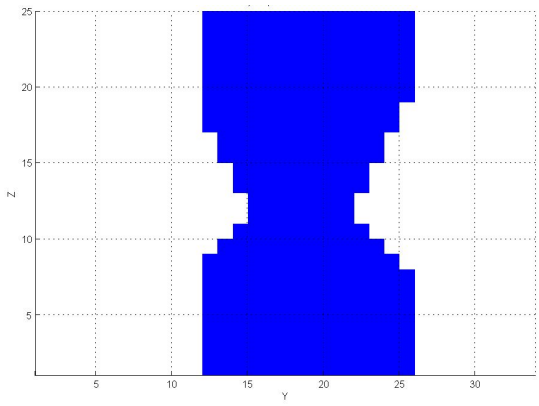

(c) Slice ZY (X=30) without convexity constraints

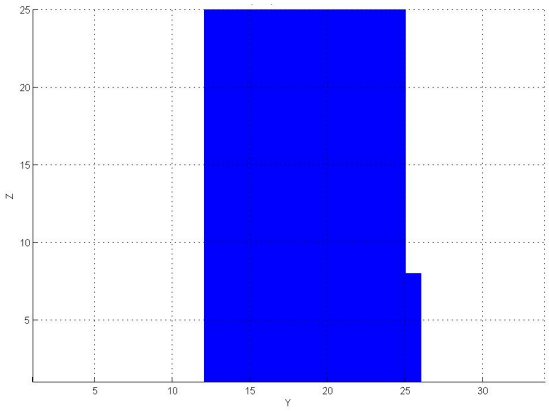

(d) Slice ZY (X=30) with convexity constraints

Figure 11: Stope shapes of both algorithms applied on deposit 1

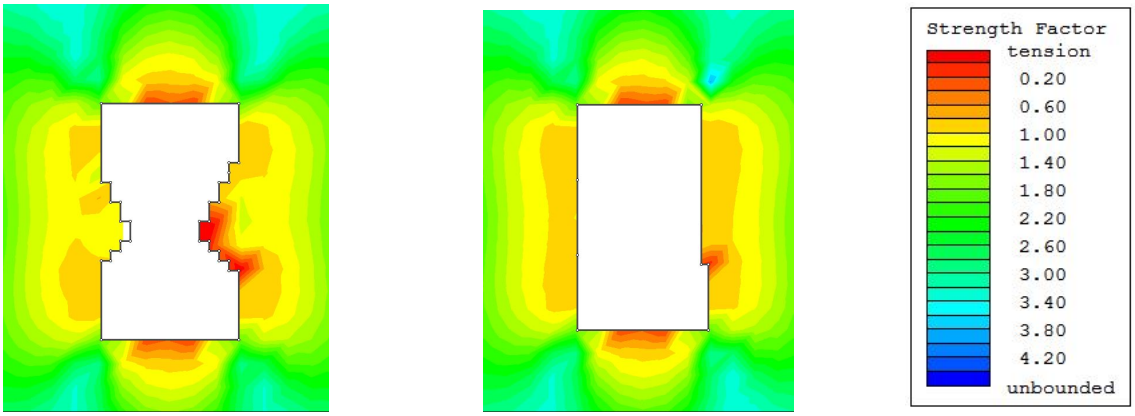

(a) Without convexity constraints

(b) With convexity constraints

Figure 12: Stability analysis of a cross-section on synthetic deposit 1. High Quality rock mass

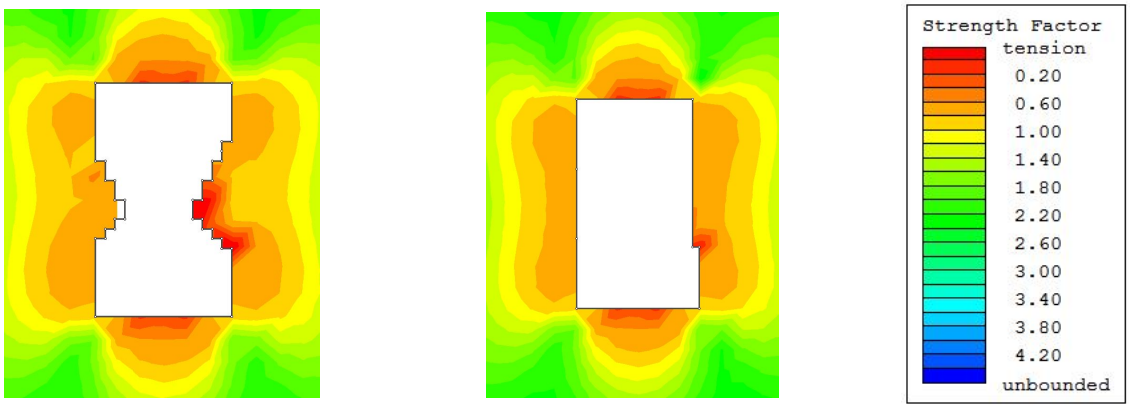

(a) Without convexity constraints (b) With convexity constraints

Figure 13: Stability analysis of a cross-section on synthetic deposit 1. Low Quality rock mass

profit), especially when compared to the impact of the discretization itself on the profit (see Table 5, deposit 1 and Table 6).

It can be noticed, also, that the new constraints structure allows the solution to add or discard blocks from the original solution obtained by Bai's methodology, depending of the value generated by these actions. This is a clear advantage over a manual adjustment stage since it is not trivial to determine whether to add or subtract blocks to achieve a better geometry, while seeking the best possible value and respecting the diagonal precedence constraints to maintain the footwall and hangingwall angles.

Regarding stability, all the new designs are more stable than their previous solutions obtained without the constraints. However, there are still some areas with lower stability despite complying with all the restrictions imposed on the formulation. This can be solved by generating smaller stopes, modifying the stope height (controlled by the raise length in the original algorithm) and the stope length (controlled by the parameter R in the original Bai's algorithm). These parameters must be selected under strict geomechanical criteria given the stress conditions and the rock mass quality where the stope will be built.

In terms of regularity of the stope design obtained by the IP formulation, we can see a great improvement in all the instances shown compared to Bai's algorithm. This will ensure an easier work for the production and construction phase in-field. However, the final stope design could be modified in real life work given the blasting control and the presence of joints or other structures.

The stope design could be further regularized using the same convexity constraints structure, but with different coordinates. For instance, in the cylindrical coordinate system, we could take rings instead of columns: the group of blocks with same r and z coordinate, but different θ. If we apply the same restrictions but changing this coordinates, we will avoid the irregularities not only vertically, but horizontally as well. This regularization will improve the stope geometry, but it will worsen the stope profit, therefore, the decision to include these new constraints will depend on the mining engineer.

As a downside, adding this new constraints would increase the variables and restrictions notably, and the instances shown are already remarkably large. Despite the low resolution times for these big instances, the definition of the instance using Gurobi requires a large amount of RAM. This is a problem in some cases, where the sole definition of variables and restrictions in Gurobi consumes all the available RAM. This is not an issue with the network structure used by Bai et al. (2013a) since it is a more compact structure, requiring less memory to be defined and solved. However, these big instances are not common in Sublevel Stoping given its selective nature. Admittedly, this issue could become a problem when multiple stopes have to be optimized simultaneously as in Bai et al. (2014).

A possible alternative to reduce the size of the instance would be the implementation of a heuristic that, instead of applying the convexity constraints in every column of the block model, focus only in its

outer columns, controlled by a parameter *pho* defined from the initial raise. From $r > pho$, this heuristic would apply the convexity constraints, leaving the inner part of the block model without these restrictions. This would take advantage of the fact that the inner parts of the block model does not present convexity issues. This heuristic could achieve good results faster than the IP-formulation and it would work with larger instances.

Finally, regarding runtimes, the IP-formulation is slower than the network structure solving the same instances, and the addition of convexity constraints increases the runtimes even more. However, this formulation remains remarkably fast for this kind of problems: the stope design definition problem belongs to the strategic mine planning stage, where decisions takes months or years to be made, so fast runtimes are not mandatory. For this reason, the IP-formulation with convexity constraints could be used in real-life applications.

5 Conclusions

The proposed methodology allows the determination of optimal stope designs, fulfilling geomechanical requirements. It generates feasible stopes in disseminated orebodies, avoiding unstable and irregular geometries. The designs comply with technical requirements such as the stope drilling pattern. The formulation can be solved in reasonable times for real life cases, and it can be extended to allow further regularization of stope design or faster resolution times using heuristics.

References

Alford C (1996) Optimisation in underground mine design. International Journal of Rock Mechanics and Mining Sciences and Geomechanics Abstracts 220A

Ataee-Pour M (2000) A heuristic algorithm to optimise stope boundaries. PhD thesis, University of Wollongong, Australia

Ataee-Pour M (2005) A critical survey of the existing stope layout optimization techniques. Journal of Mining Science 41 447–466

Bai X, Marcotte D, Simon R (2013a) Underground stope optimization with network flow method. Computers & Geosciences 52 361–371

Bai X, Marcotte D, Simon R (2013b) Incorporating drift in long-hole stope optimization using network flow algorithm. In: Proceedings of 36th APCOM, APCOM, Porto Alegre, Brasil, 391–400

Bai X, Marcotte D, Simon R (2014) A heuristic sublevel stope optimizer with multiple raises. SAIMM 114 427–434

Bieniawski Z (1989) Engineering rock mass classifications: a complete manual for engineers and geologists in mining, civil, and petroleum engineering. Wiley

Cheimanoff N, Deliac E, Mallet J (1989) Geocad: an alternative cad and artificial intelligence tool that helps moving from geological resources to mineable reserves. In: 21st Application of Computers and Operations Research in the Mineral Industry: 21st International Symposium: Papers, 471

Coulomb CA (1776) Essai sur une application des regles des maximis et minimis a quelquels problemesde statique relatifs, a la architecture. Mem Acad Roy Div Sav 7 343–387

Crouch S, Starfield A (1983) Boundary element methods in solid mechanics. George Allen & Unwin,London

Hoek H, Carranza-Torres C, Corkun B (2002) Hoek-brown failure criterion – 2002 edition. In: Proceedings of the Fifth North American Rock Mechanics Symposium (NARMS-TAC), University of Toronto Press, Toronto, 267–273

Lane K (1988) The economic definition of ore: Cut-off grades in theory and practice. Mining Journal Books,London

Laubscher DH (1990) A geomechanics classification system for the rating of rock mass in mine design. Journal of The South African Institute of Mining and Metallurgy 90 257–273

Lerchs H, Grossmann I (1965) Optimum design of open-pit mines. Transactions on CIM 58 47–54

Manchuk J, Deutsch C (2008) Optimizing stope designs and sequences in underground mines. SME Transactions 324 67–75

Mathews KE (1980) Prediction of stable excavation spans for mining at depths below 1000 m in hard rock. Report to Canada Centre for Mining and Energy Technology (CANMET),Department of Energy and Resources

Ovanic J, Young D (1995) Economic optimisation of stope geometry using separable programming with special branch and bound techniques. In: Third Canadian Conference on Computer Applications in the Mineral Industry, 129–135

Picard J (1976) Maximal closure of a graph and applications to combinatorial problems. Management Science 22 1268–1272

Riddle J (1977) A dynamic programming solution of a block-caving mine layout. In: Application of Computer Methods in the Mineral Industry: Proceedings of the Fourteenth Symposium, 767–780